

# The molecular environment of the $\text{Na}^+$ binding site of thrombin

Erli Zhang, A. Tulinsky \*

*Department of Chemistry, Michigan State University, East Lansing, MI 48824, USA*

Received 15 July 1996; revised 6 September 1996; accepted 6 September 1996

## Abstract

When  $\text{Na}^+$  binds to thrombin, a conformational change is induced that renders the enzyme kinetically faster and more specific in the activation of fibrinogen. Two  $\text{Na}^+$  binding sites have here been identified crystallographically by exchanging  $\text{Na}^+$  with  $\text{Rb}^+$ . One is intermolecular, found on the surface between two symmetry-related thrombin molecules. Since it is not present in thrombin crystal structures having different crystal systems, the other  $\text{Na}^+$  site is the functionally relevant one.

The second site has octahedral coordination with the carbonyl oxygen atoms of Arg221A and Lys224 and four conserved water molecules. It is located near Asp189 of the S1 specificity site in an elongated solvent channel ( $8 \times 18 \text{ \AA}$ ) formed by four antiparallel  $\beta$ -strands between Cys182–Cys191 and Val213–Tyr228. This channel, extending from the active site to the opposite surface of the enzyme, was first noted in the hirudin–thrombin structure and contains about 20 conserved water molecules linked together by a hydrogen bonding network that connects to the main chain of thrombin. Although the antiparallel  $\beta$ -strand interactions of the functional  $\text{Na}^+$  binding site are the same in prethrombin2, the loops between the strands are very different, so that Asp189 and Arg221A are not positioned properly for either substrate or  $\text{Na}^+$  binding in prethrombin2. A water molecule with octahedral coordination has also been identified in factor Xa at the topologically equivalent  $\text{Na}^+$  site position of thrombin. Since activated protein C shows enhanced activity with monovalent cation binding, the same position is probably utilized by  $\text{Na}^+$ . Since thrombin crystals could not be grown in the absence of  $\text{Na}^+$ , the cation was leached from  $\text{Na}^+$ -bound thrombin crystals by diffusion/exchange. Although both  $\text{Na}^+$  and their coordinating water molecules were removed from the  $\text{Na}^+$  binding sites, the remainder of the thrombin structure was, unexpectedly, the same. The lack of an allosteric change is most likely attributable to crystal packing effects. Thus, the structure of the slow form remains to be established crystallographically.

**Keywords:** Thrombin;  $\text{Na}^+$  binding; Allosteric change; Fast/slow forms

## 1. Introduction

The interaction of thrombin with fibrinogen involves binding at a fibrinogen recognition site, an

exosite that is dominated by a high population of basic residues [1–4], separate from but generally operative in concert with the active site. This binding site is also the locale for the interaction of thrombomodulin [5] heparin cofactor II [6] and thrombin platelet receptor [7]. Formation of the thrombomodulin–thrombin complex directly curtails the capacity of thrombin to convert fibrinogen to fibrin and to activate blood platelets [8,9]. Although peptide lig-

Abbreviations: PPACK-Throm, D-PheProArg chloromethyl ketone derivative of  $\alpha$ -thrombin; Hir-Throm, hirugen (sulfate Tyr63-hirudin53–64)-thrombin

\* Corresponding author.

ands specific for the fibrinogen exosite generally possess a highly anionic character, the specificity of the interaction with the site appears to reside in hydrophobic components of the ligands and thrombin [3,10–12].

Binding at the fibrinogen recognition site affects the conformational state of thrombin [13,14], its catalytic activity [15,16] and its specificity [17–19]. Although the mechanism by which binding to the fibrinogen exosite translates into structural changes at the active site remains unknown, the active site changes that occur have been determined by comparing the structures of a number of different isomorphous active site and fibrinogen exosite inhibited complexes of thrombin [20]: the conformational changes induced by exosite binding are relatively small.

It has been shown that monovalent cations bind to thrombin and enhance activity by affecting  $K_m$  and  $k_{cat}$  [21]. An important structural transition of thrombin has been identified when  $Na^+$  binding to a single site of the enzyme induces an allosteric conformational change from the slow ( $Na^+$ -free) to the fast ( $Na^+$ -bound) form [22], which is also accompanied by spectroscopic changes [23]. Under physiological conditions, the two different forms are significantly populated. The slow to fast transition is a key step of molecular recognition by thrombin, since fibrinogen binds to the fast form with higher affinity [24] and is cleaved with higher specificity while the slow form activates the anticoagulant protein C more specifically [25]. The conformational change on  $Na^+$  binding to the enzyme is also related to the allosteric regulation of the active site by the fibrinogen recognition exosite [23]. The  $Na^+$  binding site was first identified crystallographically (without much detail) in the PPACK-Throm structure, where it is located in a long water solvent channel near the S1 specificity site [26].

We present here the  $Na^+$  binding site of thrombin in Hir-Throm crystals and describe its solvent environment, which is conserved in other binary isomorphous and ternary Hir-Throm complexes inactivated at the active site. The site displays octahedral coordination involving two carbonyl oxygen atoms of the protein and four highly occupied, conserved water molecules. Since the electron density of a  $Na^+$  and a water molecule are nearly equivalent crystallographi-

cally, the site has also been identified as an octahedrally coordinated water molecule in over 20 different thrombin active site inhibited or fibrinogen exosite occupied structures (unpublished results of this laboratory). The site is near Asp189 of the specificity site of thrombin, 2/3 of the way along an elongated channel extending from an entrance close to the catalytic site (S1 specificity subsite) through the thrombin molecule to the opposite surface of the enzyme. The cylindrical-like cavity is formed by four antiparallel  $\beta$ -strands within Cys182–Cys191 and Val213–Tyr228 of the B-chain of thrombin [3,25]. The channel is further shaped by the loops/turns connecting the  $\beta$ -strands. Very significantly, the channel is occupied by about 20 water molecules [3], most of which are conserved in different thrombin structures and are linked together by a hydrogen bonding network, which ultimately connects to the main chain of the enzyme. The  $Na^+$  binding site of Hir-Throm is also compared with that of PPACK-Throm, from which it differs.

## 2. Materials and methods

Small crystals of Hir-Throm were grown by vapor diffusion methods as described previously [27] and enlarged for X-ray diffraction studies using repetitive macroseeding techniques. A solution containing equal volumes of 5 mg/ml thrombin (incubated with a 10-fold molar excess of hirugen), 0.1 M sodium phosphate buffer (pH 7.3), 0.375 M NaCl, 1 mM  $NaN_3$ , and a well solution of similar composition but with 26% PEG 8000, was equilibrated against the well solution. Small crystals appeared in about one week and were transferred as seeds to a previously equilibrated hanging drop for enlargement. The size of crystals obtained in this way ranged up to  $0.6 \times 0.3 \times 0.3$  mm; crystals were stored in a 30% PEG 8000 solution, 0.1 M phosphate buffer (pH 7.3), 0.185 M NaCl, 1 mM  $NaN_3$ .

The dissociation constants of  $Na^+$  and  $Rb^+$  with thrombin at 25°C are 22 and 350 mM respectively [22]. Crystals of Hir-Throm grown from phosphate buffer with 0.19 M NaCl are identical to those grown from 0.1 M Tris buffer, 0.2 M sodium acetate, 24% PEG 4000 with 0.19 M NaCl. Phosphate-grown crystals could be transferred to a solution of 0.1 M Tris

buffer (pH 7.3), 30% PEG 8000, 1 mM  $\text{NaN}_3$ , that was then gradually made 0.5 M in  $\text{Rb}^+$ . To minimize the sensitivity of crystals to shock in the  $\text{Na}^+/\text{Rb}^+$  exchange, they were soaked in a capillary tube used to mount crystals for diffraction [28]. The length of the capillary served to create a concentration gradient to slow down the diffusion of  $\text{Rb}^+$ . A crystal ( $0.6 \times 0.25 \times 0.25$  mm) was placed in a capillary containing 80  $\mu\text{l}$  of storage solution (0.1 M Tris buffer (pH 7.3) and 30% PEG 8000, 1 mM  $\text{NaN}_3$ ). After the crystal had settled to the bottom of the solution in the capillary, 40  $\mu\text{l}$  of solution from the top of the capillary was replaced with a solution of 0.1 M Tris buffer (pH 7.3), 30% PEG 8000, 1 mM  $\text{NaN}_3$  and 1.0 M  $\text{RbCl}$ . After soaking for 5 days, the exchange solution was removed and the capillary dried and sealed in the usual manner for X-ray diffraction purposes.

An essentially  $\text{Na}^+$ -free crystal was prepared by diffusion because thrombin crystals could not be grown in the absence of  $\text{Na}^+$ . Crystals of Hir-Throm were grown by the vapor diffusion method from a solution containing 0.1 M Tris buffer (pH 8.5), 28%

PEG4000, 0.2 M sodium acetate and 0.19 M  $\text{NaCl}$ . One of these was transferred to a capillary that contained 60  $\mu\text{l}$  of mother liquor ( $[\text{Na}^+] = 0.39$  M). Then 30  $\mu\text{l}$  of mother liquor were removed from the top of the capillary and 30  $\mu\text{l}$  of a  $\text{Na}^+$ -free solution, 0.1 M Tris buffer (pH 8.5), 35% PEG4000, were added. The procedure was repeated every 12 h until the concentration of  $\text{Na}^+$  reached  $\sim 0.2$  mM (about 4 days). Since the soaked crystal did not show observable damage, the 30–30  $\mu\text{l}$  exchange was changed to a 58–2  $\mu\text{l}$  exchange. The new procedure was repeated until the final concentration of  $\text{Na}^+$  was about 8 nM in the crystal (referred to hereafter as  $\text{Na}^+$ -free).

X-ray diffraction intensity data of Rb-Hir-Throm were collected using a Rigaku RU 200 fine focus rotating anode generator operating at 50 kV and 100 mA with an R-Axis II imaging plate detector. The crystal diffracted X-rays to about 2.1 Å resolution and belongs to the monoclinic system, space group C2, with cell parameters  $a = 71.53$  Å,  $b = 72.25$  Å,  $c = 73.26$  Å,  $\beta = 101.0^\circ$ , which are isomorphous with Hir-Throm crystals. A total of 27 769

Table 1  
Intensity data collection summary of Rb-Hir-Throm

Shell (Å)	Average intensity	Average $I/\sigma$	# of reflections		Completeness (%)		$R_{\text{merge}}$ (%)	
			Obs.	Theor.	Shell	Cumul.	Shell	Cumul.
<i>A. Rb-Hir-Throm</i>								
15.0	206	20.3	60	74	81	81	5.4	5.4
10.0	355	21.1	136	158	86	84	3.5	3.9
7.50	219	19.9	272	299	91	88	4.0	3.9
5.00	156	18.2	1098	1187	92	91	4.4	4.2
3.50	185	16.7	2884	3151	91	91	4.4	4.4
3.00	60	9.3	2369	2768	85	89	6.8	4.7
2.75	31	6.0	1760	2260	77	86	9.4	4.9
2.50	19	4.2	2277	3209	71	82	11.8	5.2
2.25	13	3.1	2820	4753	59	76	14.8	5.4
2.07	9	2.3	2179	5032	43	69	16.3	5.5
Totals			15855	22891				
<i>B. Na<sup>+</sup>-free</i>								
4.25	1162	118	2575	2627	98	98	2.8	—
3.37	816	59.2	2466	2575	96	97	4.4	—
2.95	310	22.1	2245	2549	88	94	8.3	—
2.68	169	11.5	2022	2581	78	90	11.5	—
2.48	104	6.2	1759	2558	69	86	15.3	—
2.34	89	4.2	715	2552	28	76	16.8	4.8
Totals			11782	15442				

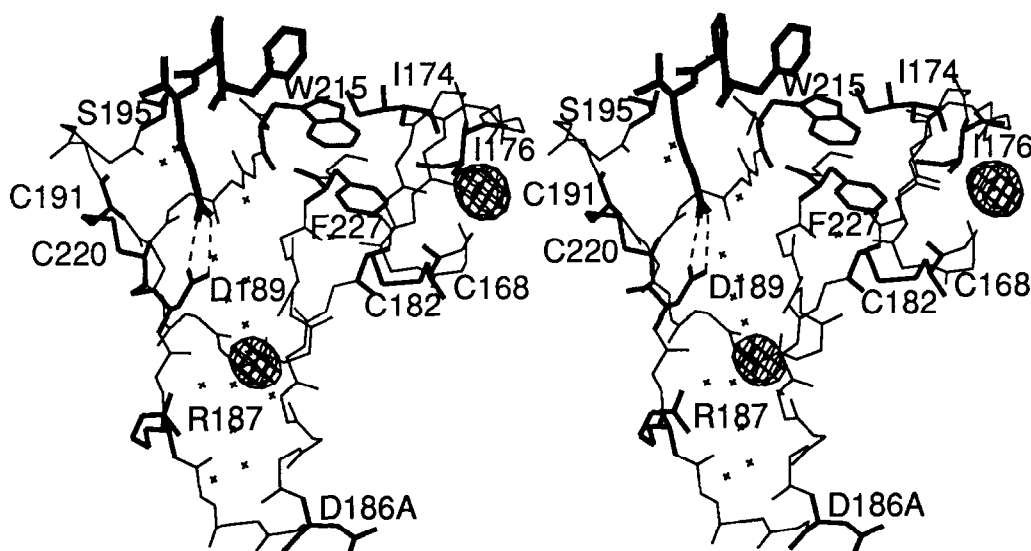


Fig. 1. Stereoview of  $\text{Na}^+$  in solvent channel in relation to the intermolecular  $\text{Na}^+$  binding site near Ile174. Difference electron density between Rb-Hir-Throm and Hir-Throm shown contoured at  $5\sigma$ . Water molecules indicated by crosses. PPACK of PPack-Throm indicated at the top entrance to the channel and selected side chains in bold; doubly hydrogen-bonded salt bridge between PPack and Asp189 of S1 site shown as broken line.

observations were measured that yielded 15 885 symmetry-independent reflections with an  $R_{\text{merge}}$  of 5.5%. Statistics relating to the intensity data collection are listed in Table 1. The observed structure amplitudes of the Rb-Hir-Throm crystal were then scaled to those of Hir-Throm.

X-ray diffraction intensity data of the  $\text{Na}^+$ -free crystal were collected using a Siemens X-1000 wire detector. The crystal diffracted to about 2.3 Å resolution (44 309 observations, 14 047 unique reflections (91%),  $R_{\text{merge}} = 4.8\%$ ) (Table 1). Furthermore, the crystal remained isomorphous with Hir-Throm crystals:  $a = 70.66$  Å,  $b = 72.47$  Å,  $c = 73.09$  Å,  $\beta = 100.7^\circ$ .

The structure of the Hir-Throm complex [27], without water molecules, was used to calculate phase angles, which were assigned to Rb-Hir-Throm and Hir-Throm amplitudes to calculate a difference electron density map. Inspection of the difference density clearly revealed two  $\text{Rb}^+$  binding sites. One was located buried in a previously reported water channel of the hirudin–thrombin complex [3] while the other was on the surface of the enzyme between crystallographically related molecules (Fig. 1). Since the latter is absent in thrombin structures having crystal forms differing from Hir-Throm, this site is the result

Table 2

Some refinement parameters and rms deviations of Rb-Hir-Throm and  $\text{Na}^+$ -free Throm<sup>a</sup>

	rms $\Delta$	Target $\sigma$
<i>Distances</i>		
Bond distance (Å)	0.014 (0.014)	0.018 (0.020)
Angle distance (Å)	0.049 (0.048)	0.038 (0.042)
Planar 1–4 distance (Å)	0.061 (0.059)	0.058 (0.065)
<i>Miscellaneous</i>		
Plane groups (Å)	0.033 (0.030)	0.040 (0.040)
Chiral centers (Å <sup>3</sup> )	0.181 (0.155)	0.150 (0.150)
<i>Non-bonded distances</i>		
Single torsion (Å)	0.23 (0.22)	0.50 (0.50)
Multiple torsion (Å)	0.30 (0.30)	0.50 (0.50)
Possible X–Y H-bond (Å)	0.26 (0.27)	0.50 (0.50)
<i>Thermal restraints</i>		
Main-chain bond (Å <sup>2</sup> )	1.7 (1.6)	2.0 (2.0)
Main-chain angle (Å <sup>2</sup> )	2.5 (2.5)	2.5 (2.5)
Side-chain bond (Å <sup>2</sup> )	3.0 (2.7)	3.0 (3.0)
Side-chain angle (Å <sup>2</sup> )	4.0 (3.9)	3.5 (3.5)

Diffraction pattern:  $\sigma(I_{\text{Fo}}) = 5.4 - 30[(\sin \theta / \lambda) - 1/6]$ ,  $(\sigma(I_{\text{Fo}})) = 1.4 - 12[(\sin \theta / \lambda) - 1/6]$ ,  $\langle \|F_{\text{Fo}}\| - \|F_{\text{c}}\| \rangle = 10.4$ ,  $\langle (\|F_{\text{Fo}}\| - \|F_{\text{c}}\|) \rangle = 2.8$ ,  $\langle B \rangle = 31$  Å<sup>2</sup>,  $\langle \langle B \rangle \rangle = 27$  Å<sup>2</sup>.

<sup>a</sup>  $\text{Na}^+$ -free thrombin in parentheses.

of intermolecular crystal packing in the monoclinic crystals, space group C2. Thus, the  $\text{Na}^+$  site in the water channel is the site that affects thrombin catalytic competency.

The Hir-Throm structure was energy minimized using X-PLOR and then refined by restrained least-squares procedures with the program PROLSQ. The diffraction data included in refinement were from 7.0–2.0 Å with a  $3.0\sigma$  cutoff on  $|F|^2$ . During the refinement, two  $\text{Rb}^+$  and 125 water molecules were also fitted to the (2Fo–Fc) and (Fo–Fc) maps. The final model has an *R*-factor of 15.1%; a summary of the refinement parameters is given in Table 2. The  $\text{Na}^+$ -free Hir-Throm structure was refined similarly at 2.3 Å resolution (137 water molecules) converging at *R* = 14.9% (Table 2). The coordinates of the Rb-Hir-Throm and  $\text{Na}^+$ -free Hir-Throm structures have been deposited in the Brookhaven Protein Data Bank (access numbers 1HXE and 1HXF, respectively).

### 3. Results and discussion

The functional and physiologically important  $\text{Na}^+$  binding site is located in a conspicuous water channel first observed in the hirudin–thrombin structure [3], including and extending off the S1 specificity site of thrombin (Fig. 1). The elongated cylindrical tunnel is formed by three antiparallel  $\beta$ -strands (Met180–Tyr184A, Val213–Gly219, Lys224–Tyr228; strands 1, 3, 4) crossed diagonally by Gly188–Glu192 (strand 2) with Asp189 of the S1 specificity site near the midpoint [3,25]. Most of this region is within the part of the activation domain of prethrombin2, and presumably that of prothrombin also, that leads to the formation of the S1 specificity pocket [20]. The 8 Å diameter channel traverses about 18 Å of the thrombin molecule from the catalytic site to the opposite surface of the molecule. One wall of the channel is abundant in aromatic residues (Tyr184A, Trp215, Tyr225, Phe227, Tyr228), which contrasts with the other wall lined by hydrophilic residues (Fig. 1). The channel is filled with over 20 water molecules linked together by a hydrogen bonding network that also connects up to the protein (Fig. 2). Most of this water is conserved in different thrombin structures and corresponds to high occu-

pancy factors (Table 3). The entrances to the channel are the S1 specificity site on one side and a hole in the thrombin surface on the other, the latter lined with the residues of the Gly186A–D insertion loop. The water structure above and below the  $\text{Na}^+$  in the channel can be conveniently subdivided into three regions: (I) that from Asp189 in the S1 site to the entrance near the catalytic site; (II) that between the  $\text{Na}^+$  octahedral square plane containing Arg221AO, Lys224O,  $\text{O}_{\text{w}}416$ ,  $\text{O}_{\text{w}}445$  up to Asp189; and (III) that between this plane and the other entrance to the water channel at the 186A–D surface (Fig. 2).

#### 3.1. Region II: the $\text{Na}^+$ site

In the Hir-Throm structure [20],  $\text{O}_{\text{w}}409$  with an occupancy of 1.0 and a *B*-value of  $13 \text{ \AA}^2$  has been identified to be the  $\text{Na}^+$ , by replacement with  $\text{Rb}^+$ , responsible for the slow to fast transition. The superposition of the difference electron density near the  $\text{Na}^+$  site between Rb-Hir-Throm and Hir-Throm, calculated with Hir-Throm phases less water structure, on the omit map of Hir-Throm, calculated without  $\text{O}_{\text{w}}409$  and its coordinating waters in the model structure, is shown in Fig. 3a. Although the position of the  $\text{Rb}^+$  difference peak is displaced about 1.6 Å from the  $\text{Na}^+$ , the difference is decreased by half after refinement of the Rb-Hir-Throm structure. The occupancy at this  $\text{Rb}^+$  is 0.45 (*B* =  $38 \text{ \AA}^2$ ) while that of the other  $\text{Rb}^+$ , bound between two neighboring molecules, is comparable at 0.52 (*B* =  $23 \text{ \AA}^2$ ). The partial occupancy of the  $\text{Rb}^+$  is related to the larger dissociation constant (~16 fold) compared to  $\text{Na}^+$ .

The  $\text{Na}^+$  in the water solvent channel is octahedrally coordinated in Hir-Throm by the carbonyl oxygen atoms of Arg221A and Lys224 and four conserved water molecules ( $\text{O}_{\text{w}}416$ ,  $\text{O}_{\text{w}}419$ ,  $\text{O}_{\text{w}}445$ ,  $\text{O}_{\text{w}}447$ ) (Fig. 2, Tables 3 and 4). The Asp189 residue of the S1 specificity site is located adjacent to  $\text{O}_{\text{w}}447$  (Asp189OD1– $\text{O}_{\text{w}}447$ , 3.6 Å). This particular water molecule of the  $\text{Na}^+$  site hydrogen bonds to  $\text{O}_{\text{w}}427$ , which, like  $\text{O}_{\text{w}}423$ , is tetrahedrally coordinated (Gly188O,  $\text{O}_{\text{w}}447$ ,  $\text{O}_{\text{w}}405$ ,  $\text{O}_{\text{w}}416$ ). The water  $\text{O}_{\text{w}}423$  is close to  $\text{O}_{\text{w}}447$  (3.7 Å) of the  $\text{Na}^+$  site and is fully hydrogen bonded with Glu217O, Asp221N, Arg221AN and  $\text{O}_{\text{w}}494$ . Thus, both of these water molecules ( $\text{O}_{\text{w}}423$ ,  $\text{O}_{\text{w}}427$ ) have full four coordina-

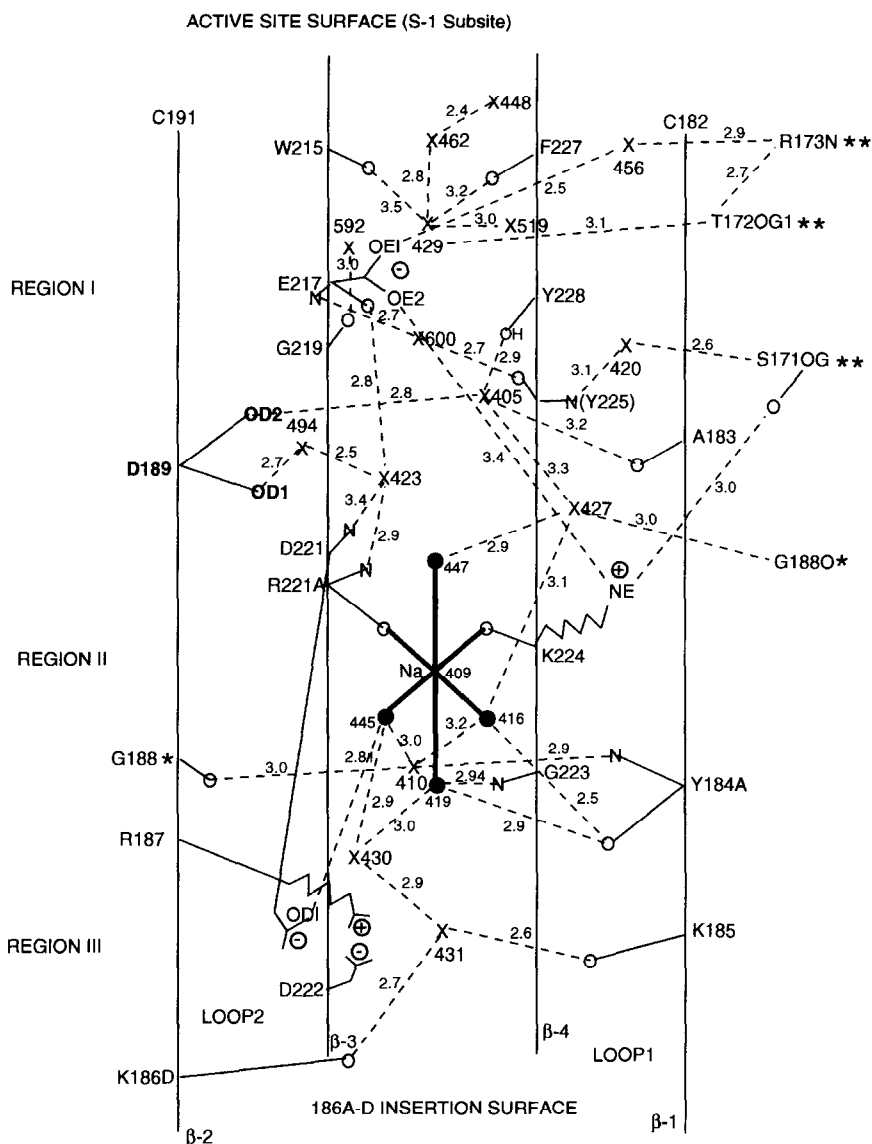


Fig. 2. Position of the  $\text{Na}^+$  site in, and interactions of conserved water molecules (designated by X) of, the water solvent channel. Single asterisk denotes location on  $\beta$ -2; double asterisk: do not occur on any of the four  $\beta$ -strands; 2.4–3.1 Å generally used as hydrogen bond criterion.

tion and ultimately link to the peptide backbone of thrombin through hydrogen bonds (Fig. 2 and Table 3).

Of the remaining water molecules at the  $\text{Na}^+$  site,  $\text{O}_w416$  hydrogen bonds directly with Tyr184AO,  $\text{O}_w410$  and  $\text{O}_w427$ . It is thus also tetrahedrally coordinated. The remaining two water molecules of the

$\text{Na}^+$  coordination sphere ( $\text{O}_w419$ ,  $\text{O}_w445$ ) both hydrogen-bond to  $\text{O}_w430$ , which hydrogen-bonds with  $\text{O}_w431$  and is located near the positive/negative centers of the bidentate Arg187–Asp221–Asp222 salt bridge (Figs. 2 and 4). The  $\text{O}_w445$  of the  $\text{Na}^+$  site also bridges to Asp221OD1 and  $\text{O}_w410$  (then  $\text{O}_w410$  back to Tyr184AN). The  $\text{O}_w419$  forms addi-

Table 3

Water molecules in the solvent channel of Hir-Throm and monoclinic PPACK-Throm

Hir-Throm					Monoclinic PPACK-Throm [20]			
O <sub>w</sub>	Occup.	B (Å <sup>2</sup> )	(Occ) <sup>2</sup> /B (Å <sup>-2</sup> × 10 <sup>2</sup> )	Coordination number	O <sub>w</sub>	Occup.	B (Å <sup>2</sup> )	(Occ) <sup>2</sup> /B (Å <sup>-2</sup> × 10 <sup>2</sup> )
<i>Region I</i>								
405	1.00	13	7.8	4	403	1.00	12	8.4
420	1.00	21	4.7	3	409	0.99	19	5.2
423	1.00	21	4.9	4	417	1.00	15	6.6
429 <sup>a,b</sup>	1.00	25	4.1	4	407 <sup>a</sup>	0.98	17	5.7
448 <sup>b</sup>	0.91	26	3.2	1		displaced		
462 <sup>b</sup>	0.82	29	2.3	2		displaced		
494	0.71	37	1.4	2	521	0.64	43	1.0
519 <sup>b</sup>	0.62	25	1.6	1		displaced		
592 <sup>a,b</sup>	0.50	23	0.9	4	428	0.98	22	4.4
600	1.00	20	5.0	2	509	0.30	15	0.6
<i>Region II</i>								
409(Na <sup>+</sup> )	1.00	13	7.6	6	410(Na <sup>+</sup> )	1.00	21	4.7
410	1.00	17	5.8	4	514	0.47	36	0.6
416 <sup>c</sup>	1.00	20	5.1	4	450	0.59	22	1.6
427	1.00	26	3.9	4	448	0.75	25	2.3
445 <sup>c</sup>	0.94	26	3.4	4	418	0.92	20	4.5
447 <sup>c</sup>	0.93	22	4.0	2	433	0.87	29	2.6
<i>Region III</i>								
419 <sup>c</sup>	1.00	21	4.8	4	424	0.81	23	2.9
430	1.00	26	3.9	3	482	0.81	21	3.2
431	1.00	2.5	4.0	3	464	0.98	32	3.1

<sup>a</sup> O<sub>w</sub>429 shifted 0.4 Å. O<sub>w</sub>592 shifted 1.0 Å with PPACK binding.<sup>b</sup> In S1 specificity site.<sup>c</sup> Coordinates Na<sup>+</sup>.

tional hydrogen bonds with Tyr184AO and Gly223N. The Na<sup>+</sup> bridges directly to the peptide chain (Arg221A, Lys224) and its water coordination sphere does likewise indirectly through a complex hydrogen-bonded network mediated by other conserved water molecules (Fig. 2 and Table 3). Of the four water molecules coordinating the Na<sup>+</sup>, three exhibit full four coordination, mostly through hydrogen bonds (O<sub>w</sub>447 also is four coordinated if the longer 3.6 Å contact with Asp189OD1 is considered).

The Rb<sup>+</sup> in the solvent channel differs from the Na<sup>+</sup> in that it appears to have distorted square bipyramidal eight-fold coordination (square and distorted square, tetragonal pyramids emanating from the Rb<sup>+</sup>) (Fig. 3b, Table 4). This is most likely due to its larger ionic radius (Na<sup>+</sup> ~ 1.0 Å, Rb<sup>+</sup> ~ 1.5 Å), which is responsible for the positional shift and generally leads to the longer contacts with oxygen. The shifted Rb<sup>+</sup> expels O<sub>w</sub>416 of the Na<sup>+</sup> site,

producing an additional direct contact with thrombin to Tyr184AO (Fig. 3b, Table 4), an interaction also observed in the orthorhombic Rb-PPACK-Throm structure [26]. The coordination is completed with five water molecules, three of which are in common with the Na<sup>+</sup> site. The O<sub>w</sub>519 of the Rb<sup>+</sup> site is a shifted O<sub>w</sub>447 of the Na<sup>+</sup> site (~ 1.4 Å) where it is the closest Na<sup>+</sup> contact (Table 4). The two new water molecules (O<sub>w</sub>520, O<sub>w</sub>538) of the Rb<sup>+</sup> site are O<sub>w</sub>410 and O<sub>w</sub>427 of the solvent channel that are located close to the Na<sup>+</sup> site (Fig. 2).

Specific monovalent cation effects in blood coagulation were first reported for factor Xa [29] and then for thrombin [21] and activated protein C [30]. Examination of the structure of factor Xa [31] in the vicinity of the Na<sup>+</sup> site of thrombin reveals that O<sub>w</sub>583 of factor Xa is at the Na<sup>+</sup> position and is octahedrally coordinated by topologically equivalent Arg222O (Arg221AO of thrombin) and Lys224O

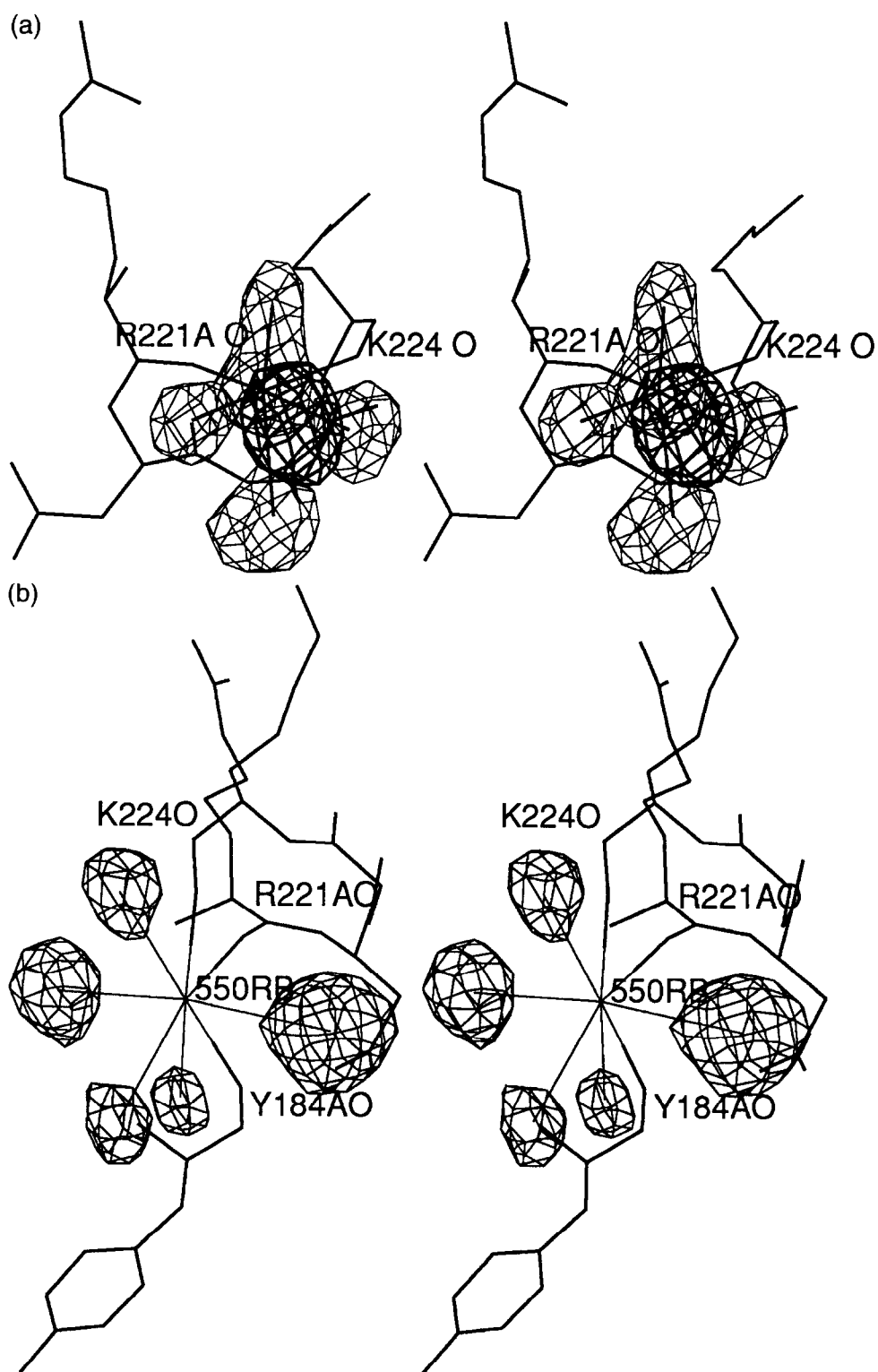




Table 4

Coordination of  $\text{Na}^+$  and  $\text{Rb}^+$  in thrombin and factor Xa  
A. Kinetically functional site

Hir-Throm (mono)	$d$ (Å)	PPACK- Throm (mono)	$d$ (Å)	$\text{Rb}^+$ -Hir- Throm (mono)	$d$ (Å)
Arg221AO	2.48	Arg221AO	2.41	Arg221AO	2.98
Lys224O	2.34	Lys224O	2.24	Lys224O	2.68
$\text{O}_{\text{w}}416$	2.59	$\text{O}_{\text{w}}450$	2.72	Tyr184AO	3.49
$\text{O}_{\text{w}}419$	2.86	$\text{O}_{\text{w}}424$	2.70	$\text{O}_{\text{w}}469$	3.52
$\text{O}_{\text{w}}445$	2.41	$\text{O}_{\text{w}}418$	2.63	$\text{O}_{\text{w}}537$	3.02
$\text{O}_{\text{w}}447$	2.05	$\text{O}_{\text{w}}433$	2.06	$\text{O}_{\text{w}}519$	3.38
				$\text{O}_{\text{w}}520$	3.09
				$\text{O}_{\text{w}}538$	3.26

## B. Factor Xa

$\text{Na}^+$ site	$d$ (Å)
Tyr185O	2.1
Asp185AO	2.6
Arg222O	2.0
Lys224O	2.5
$\text{O}_{\text{w}}672$	3.1
$\text{O}_{\text{w}}741$	2.2

## C. Intermolecular site

Hir-Throm	$d$ (Å)	$\text{Rb}^+$ -Hir-Throm	$d$ (Å)
Lys169O	2.54	Lys169O	2.92
Thr172O	2.36	Thr172O	2.86
Phe204AO <sup>a</sup>	2.37	Phe204AO <sup>a</sup>	2.60
$\text{O}_{\text{w}}432$	2.67	$\text{O}_{\text{w}}541$	3.36
$\text{O}_{\text{w}}610$	2.40	$\text{O}_{\text{w}}542$	2.98 <sup>b</sup>
$\text{O}_{\text{w}}611$	2.38	$\text{O}_{\text{w}}540$	2.96 <sup>b</sup>

<sup>a</sup> From crystallographically adjacent molecule.

<sup>b</sup> Occupancy < 0.5.

(Table 4). Thus, this assumed water molecule in the factor Xa structure is most likely a  $\text{Na}^+$ . The exact composition of the site differs from thrombin. The different side-chain structure of factor Xa leads to four carbonyl oxygen atoms from the protein coordinating with the  $\text{Na}^+$  (Table 4). The oxygen atoms of Tyr185O, Arg222O, Lys224O and  $\text{O}_{\text{w}}741$  are in an approximate plane with Asp185AO and  $\text{O}_{\text{w}}672$  at the apices of the octahedral array. Since activated

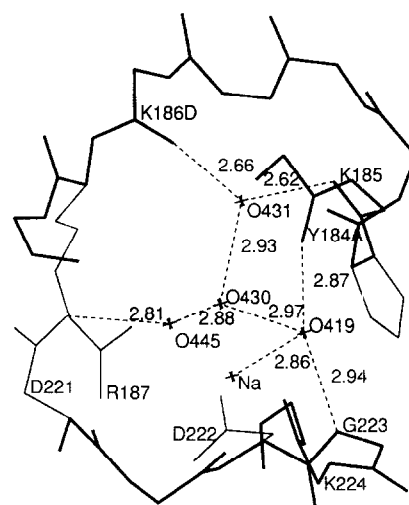


Fig. 4. Geometry of entrance to the solvent channel from the 186 A–D insertion loop region.

protein C also shows kinetic enhancement with monovalent cation binding [30,32], it most likely has a similar  $\text{Na}^+$  binding site to thrombin and factor Xa.

## 3.2. Region III

One entrance to the  $\text{Na}^+$ -containing solvent channel is at the S1 specificity site of thrombin. Region III is located on the opposite end of the channel and forms the other entrance. The two loops between the  $\beta$ -strands of the channel line the entrance: loop 1 (Lys185–Arg187) contains the 186A–D insertion and connects strands 1 and 4; and loop 2, between Asp221–Lys224, connects strands 2 and 3 of the channel with a Type I  $\beta$ -turn (Arg221A–Lys224). There are three conserved water molecules in the region. One is the apical  $\text{O}_{\text{w}}419$  of the  $\text{Na}^+$  octahedron while the others are the previously mentioned  $\text{O}_{\text{w}}430$  and  $\text{O}_{\text{w}}431$ . The  $\text{O}_{\text{w}}419$  bridges between loops 1 and 2 by hydrogen bonding with Tyr184AO and Gly223N (Fig. 4). The  $\text{O}_{\text{w}}430$  mediates the two loops through  $\text{O}_{\text{w}}419$  near the Arg187–Asp221–

Fig. 3. Stereoview of kinetically functional  $\text{Na}^+$  binding site. (a) Difference density between  $\text{Rb}^+$  and  $\text{Na}^+$  site contoured at  $6.5\sigma$  in bold; omit map of  $\text{Na}$ -Hir-Throm without the five waters of the  $\text{Na}^+$  site included; contoured at  $3.5\sigma$ . (b) Omit map of  $\text{Rb}$ -Hir-Throm without five  $\text{Rb}^+$  coordinating water molecules included in model; contoured at  $2.8\sigma$ .

Asp222 salt bridge, and  $O_w431$  hydrogen-bonds between Lys185O and Lys186DO to additionally firmly stabilize loop 1.

Viewing this entrance to the channel from the solvent reveals that the three water molecules are centrally located. The  $O_w431$  connects strands 1 and 2 indirectly with the aid of an ion pair,  $O_w430$  links strands 2 and 3, the  $Na^+$  bridges strands 3 and 4 through Arg221AO and Lys224O, while  $O_w419$  connects strands 1 and 4 (Fig. 4). Thus the  $Na^+$  site and accompanying conserved water molecules of regions II and III of the channel stabilize, if not organize, this end of the channel and the four  $\beta$ -strands of the fast form of thrombin. The highly coordinated and hydrogen-bonded nature of the water molecules at this entrance probably mitigate against an easy indiscriminate penetration and exchange of other molecules from the solvent.

The reorganization of the water network to the slow form of thrombin, with the release of  $Na^+$  from its site, was the object of the diffusion exchange experiment that produced the  $Na^+$ -free Hir-Throm crystal. The final (2Fo–Fc) electron density map of the  $Na^+$ -free crystal showed that both  $Na^+$  ions were indeed leached out of the crystal along with three of the water molecules coordinating the  $Na^+$  site ( $O_w416$ ,  $O_w445$ ,  $O_w447$ ) (Fig. 2). Surprisingly, however, except for minor movements of Arg221A and Lys224 ( $< 0.25 \text{ \AA}$ ), which coordinate the  $Na^+$ , the remainder of the structure was essentially undisturbed and was basically identical to that of Hir-Throm ( $rms \Delta = 0.20 \text{ \AA}$  for  $C_\alpha$  CN atoms). The same applies to the intermolecular  $Na^+$  site region. The presence of Pro225 in trypsin reorients Lys224O by  $90^\circ$  ( $\Delta = 2.4 \text{ \AA}$ ), which then forms a hydrogen bond with a water molecule positionally identical to  $O_w447$ . This movement could conceivably be the trigger for  $Na^+$  release (E. DiCera, personal communication). Except for the three aforementioned water molecules, only one other water of the solvent channel ( $O_w456$ ) was missing, so that 14 of the 18 water molecules of Fig. 2 and Table 3 are preserved in the  $Na^+$ -free structure. In view of its profound functional differences, the slow form of thrombin must have a different structure than the fast form; but since that of the leached  $Na^+$ -free Hir-Throm structure is the same, it suggests that the crystal packing arrangement may have prevented the allosteric

change from taking place upon leaching out the  $Na^+$ . Although hirudin induces the slow to fast transition and can stabilize the fast form in the absence of  $Na^+$  [23], the effect is not a factor in the case of Hir-Throm. Thus the structure of the slow form remains to be established crystallographically. Considering the intricacy of the water molecule network around the  $Na^+$  site (Fig. 2), the allosteric reorganization between the two forms should be expected to be substantial. The Asp221–Arg221A–Asp222 to Ala221–Arg221A–Lys222 (ARK) mutant of thrombin loses its ability to bind  $Na^+$  selectively and it has been suggested to have a conformation that is functionally and structurally intermediate between the slow and fast forms of the wild type [26]. Preliminary crystallographic results indicate that the structure of the ARK mutant of Hir-Throm differs in the allosteric  $Na^+$  site region from that of Hir-Throm (unpublished results of this laboratory).

### 3.3. Region I

Some of the water structure of the active site region of Hir-Throm and the isomorphous monoclinic form of PPACK-Throm have been compared previously [20]. Of the 15 water molecules in the region, about eight are expelled with PPACK binding. However, 12 water molecules are found in the region in the monoclinic form of PPACK-Throm because five new water molecules bind around the solvent-accessible surface of the inhibitor.

There are three other conserved water molecules of high occupancy in the region:  $O_w405$ ,  $O_w423$ ,  $O_w427$ . Strands 1, 2 and 4 of the cavity are bridged by  $O_w405$ , which displays nearly tetrahedral geometry by hydrogen bonding with Asp189OD2 ( $\beta$ -2) and Tyr228OH( $\beta$ -4) and by being close to Ala183O ( $\beta$ -1) and  $O_w427$  (3.2 and 3.3  $\text{\AA}$ , respectively). A similar geometry is found around previously mentioned  $O_w423$  that bridges  $\beta$ -2 and  $\beta$ -3 with the help of  $O_w494$ : Asp189OD1 ( $\beta$ -2),  $O_w494$ , Glu217O ( $\beta$ -3), Asp221N ( $\beta$ -3) and Arg221AN ( $\beta$ -3). In addition, strands 3 and 4 are connected by hydrogen bonds from  $O_w600$  to Glu217N ( $\beta$ -3) and Tyr225O ( $\beta$ -4). Thus the side chain of the all-important Asp189 residue in the specificity pocket is stabilized by a complicated hydrogen-bonding network and sits positionally poised, with no or minimal movement

required, to form a doubly hydrogen-bonded salt bridge with an arginyl guanidinium group of substrate (Fig. 5). Furthermore, the four  $\beta$ -strands at this end of the solvent channel appear to be held in place by these water molecules, similar to the other entrance of the channel. Since these features are conserved in all thrombin structures, the water hydrogen bonding network can be thought of as an integral part of the molecular structure of the enzyme. Such conservation should be of use in improving binding in the rational design of antithrombotic drugs.

The upper reaches of region I terminate with a water cluster that is found centrally located in the S1 specificity site of Hir-Throm:  $O_w429$ ,  $O_w448$ ,  $O_w462$ ,  $O_w519$  [20]. The last three are expelled when S1 is occupied by an arginyl or comparably sized side chain;  $O_w429$ , however, shifts in position by about  $0.5 \text{ \AA}$  (it is  $O_w407$  in PPACK-Throm) and helps anchor the guanidinium group of the arginyl by hydrogen-bonding with one of the  $NH_2$  groups and bridging to Phe227O through another hydrogen bond (Fig. 5). This bridging water molecule has been observed in other arginyl and lysyl-related P1 derivatives of thrombin [33]. The other  $NH_2$  group is firmly hydrogen-bonded to Gly219O. Another water molecule in the specificity site,  $O_w592$ , moves on

substrate binding (shifts about  $1.0 \text{ \AA}$  and appears to be  $O_w428$  in PPACK-Throm) [20]. The guanidinium group of the arginyl is further stabilized by this shifted water molecule that hydrogen bonds with the NE atom and Glu192OE1, Gly216O, Gly219O, also observed elsewhere [33]. Thus not only is the Asp189 residue held firmly for binding but also the guanidinium group of the substrate after binding, through a double hydrogen-bonded salt bridge and interactions anchoring it directly back to the protein through hydrogen-bonded water molecules (Fig. 5). This impressive water-mediated structure in the vicinity of the arginyl S1 salt bridge is conserved in most, if not all, arginyl P1 substrate thrombin complexes.

### 3.4. Disulfide bridges

Three of the four disulfide bridges of thrombin straddle the solvent cavity and the active site (Cys42–Cys58, Cys168–Cys182, Cys191–Cys220) and may be a hallmark of the structural integrity of the region (Fig. 1). The Cys191–Cys220 bridge is conspicuous in that it connects the  $\beta$ -2 and  $\beta$ -3 strands of the cavity and is adjacent to and only about  $5.0 \text{ \AA}$  from Asp189, stabilizing the S1 specificity site. In arginyl-like substrate complexes (Fig.

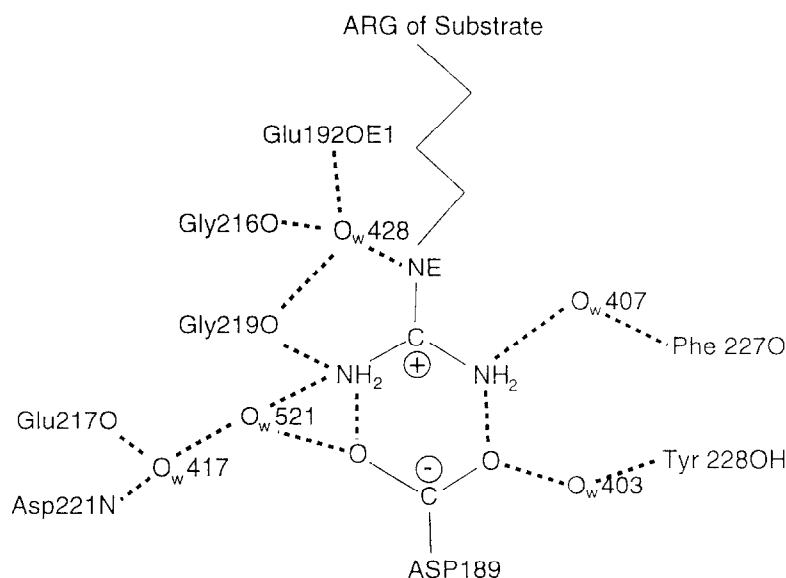


Fig. 5. Conserved salt bridge and hydrogen-bonding interactions of arginyl group bound in S1 specificity site of PPACK-Throm. Hydrogen bonds dotted.

5), the residues on either side of Cys220 make close contacts with Asp189 (Asp221N through two water molecules and the guanidinium group of substrate to Gly219O). The Cys168–Cys182 disulfide is indirectly associated with the aromatic wall of the cavity adjacent to a hydrophobic cluster (Val167, Ile174, Ile176) that forms part of the S3 D-Phe subsite of PPACK-Throm. The Ile174 residue has a prominent role interacting with groups bound at this site. The Cys42–Cys58 disulfide bridge appears to be important not only in positioning His57 at the catalytic site but also in constricting a potentially unwieldy surface  $\beta$ -strand between these cysteine residues.

### 3.5. The Glu217Ala mutation in thrombin

Mutation of Glu217 of thrombin to alanine decreases the catalytic efficiency of fibrinopeptide A activation 40-fold, while the affinity of the mutant for thrombomodulin-dependent protein C activation is reduced by only 50% [34]. Thus the mutant thrombin behaves in an enhanced anti-coagulant manner in bleeding situations comparable to the  $\text{Na}^+$ -free, slow form of thrombin [24,25]. Since Glu217 is conserved in thrombin from nine vertebrate species [35] and the P5 glycine residue of fibrinogen is generally conserved [34,36], it was suggested that the interaction observed between these two residues is required for full procoagulant function [34]. In the crystal structures of fibrinopeptide A complexed with thrombin [36,37], and the Ser195Ala mutant of thrombin (unpublished results of this laboratory) Glu217 makes only one marginal van der Waals contact with the P5 glycine residue (3.4 Å; moreover, between atoms that are not pointed at each other). It is difficult to understand how such a tenuous minor contact can be of such importance in mediating the pro- and anti-coagulant behavior of the enzyme. However, since Glu217OE2 makes a salt bridge with Lys224NE (Fig. 2), and since the latter binds directly to the  $\text{Na}^+$  that mediates fast/slow thrombin kinetics, the Glu217Ala mutation most likely adversely affects or possibly destroys the  $\text{Na}^+$  binding site that results in the favorable anticoagulant behavior [34]. Mutation of Lys224 to alanine leads to a thrombin with kinetic properties similar to the Glu217Ala mutant (E. Di Cera, personal communication). The salt bridge between Glu217 and Lys224 is crucial in maintaining

the relative positions of strands  $\beta$ -3 and  $\beta$ -4 (Fig. 2), which most likely is also important for producing the  $\text{Na}^+$  binding site. Although it was argued that the effects of the  $\text{Na}^+$  transition and the effects of the Glu217Ala mutation on catalytic efficiency of fibrinopeptide A release (7-fold versus 40-fold) and on affinity for thrombomodulin (4.4 versus 0.5-fold) are different [34], the mutant enzyme was studied under different solution conditions and at 37°C rather than 25°C, thus detracting from the comparison.

Furthermore, the Glu217O atom hydrogen-bonds with  $\text{O}_{w423}$ , which in turn forms hydrogen bonds with Asp221N and Arg221AN (Fig. 2). It has already been shown that mutation of the Asp221Arg221AAsp222 triplet to ARK leads to loss of  $\text{Na}^+$  binding [26], so disruption of this hydrogen bonding network could also lead to a state intermediate between the  $\text{Na}^+$ -bound and  $\text{Na}^+$ -free forms and account for the kinetic behavior of the Glu217Ala mutant without recourse to the P5 substrate Glu217 interaction.

### 3.6. Intermolecular $\text{Na}^+$ binding site

The  $\text{Rb}^+$  exchange experiment also revealed a second  $\text{Na}^+$  binding site in Hir-Throm. The site is located on the surface between two crystallographically symmetry-related (2-fold rotation) thrombin molecules. The  $\text{Na}^+$  is octahedrally coordinated by Lys169O and Thr172O of one molecule, Phe204AO of another, and three water molecules (Fig. 6, Table 4). Like the  $\text{Na}^+$  site in the solvent cavity, this particular site is present in nearly all Hir-Throm derivative C2 structures, generally as an octahedrally coordinated water molecule. Before the  $\text{Rb}^+$  exchange experiment, however, we had interpreted this region in Hir-Throm crystals in terms of the position of the side chain of Arg15 of the A-chain of thrombin with  $\text{NH}_2$  at the  $\text{Na}^+$  position [20]. This is now obviously incorrect. Since this intermolecular site remains octahedral on exchange with  $\text{Rb}^+$  (Table 4), it would suggest that the eight-fold  $\text{Rb}^+$  coordination of the  $\text{Rb}^+$  in the  $\text{Na}^+$  site may be the result of crowding the larger ion into the inflexible, highly conserved and energetically stabilized water channel. The direct contacts with the eight coordinate  $\text{Rb}^+$  also suggest this by corresponding to an inner (< 3.0 Å) and an outer ( $\sim 3.5$  Å) coordination sphere (Table 4).

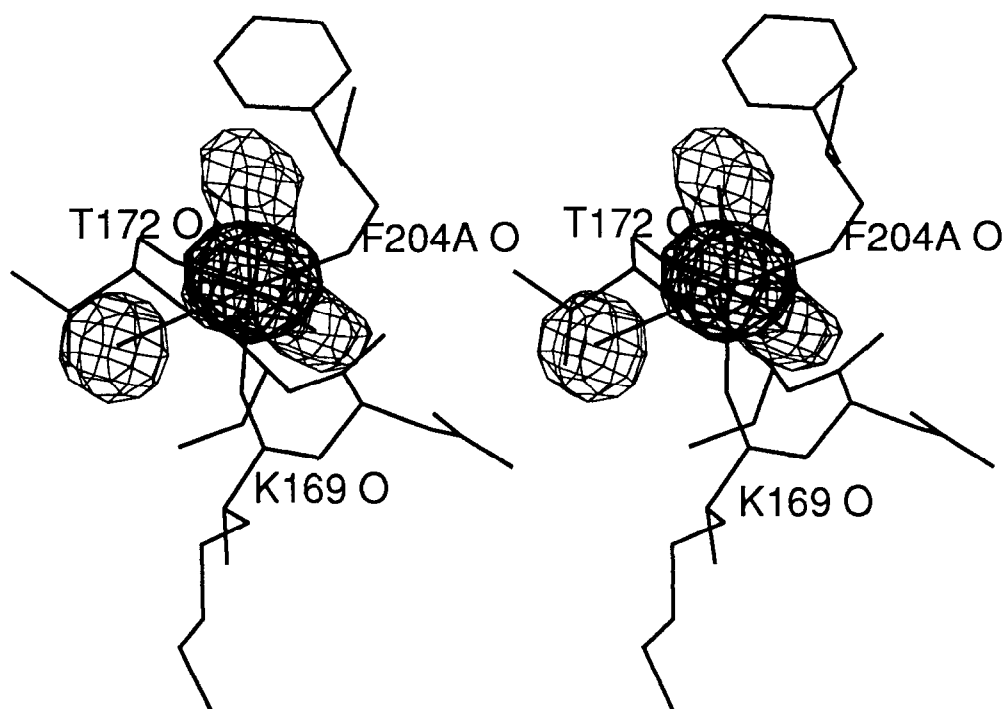


Fig. 6. Stereoview of intermolecular  $\text{Na}^+$  binding site of monoclinic crystals of Hir-Throm and derivatives. Maps as in Fig. 3(a) but contoured at  $8.0$  and  $3.0\sigma$  respectively. Phe204A corresponds to a crystallographically related molecule.

The question of whether this binding site is inherent to the thrombin molecule or whether it is just an intermolecular crystal structure packing interaction has been resolved by examining the Lys169, Thr172, Phe204A positions in thrombin crystal structures with different packing arrangements. This includes the crystal structures of (1)  $\gamma$ -thrombin [38] and the complexes of (2) orthorhombic PPACK-Throm [4], (3) hirudin-thrombin [3], (4) prothrombin kringle 2-thrombin [39], (5) DNA-15mer-thrombin [40,41] and (6) a thrombomodulin peptide-thrombin complex [12]. The second  $\text{Na}^+$  binding site was either not involved in an intermolecular contact or was different in all of these crystal structures except for possibly the thrombomodulin peptide-thrombin complex, so the site is probably not present in the solution structure of thrombin. It does, however, appear to be important for the growth of the monoclinic C2 crystals of Hir-Throm because it occurs in all of them. The crystals of the thrombomodulin peptide-thrombin complex are tetragonal, space group  $\text{P4}_3$ , two complexes per asymmetric unit, and,

surprisingly, have an identical intermolecular  $\text{Na}^+$  contact with a water molecule located at the  $\text{Na}^+$  position. No other water molecules appear in the vicinity, but this could be due to the lower resolution ( $3.0 \text{ \AA}$ ) of the structure determination. Factor Xa also displays a crucial intermolecular packing interaction in crystals where the arginyl of the C-terminal cleavage site of the activation peptide of one molecule binds in the S1 specificity site of a neighboring molecule [31]. The interaction is so important that it has not yet been possible to crystallize factor Xa in another crystal system or space group.

### 3.7. Absence of the $\text{Na}^+$ site in prethrombin2

The antiparallel  $\beta$ -strand interactions of the kinetically functional  $\text{Na}^+$  binding site of thrombin are the same in the zymogen precursor prethrombin2 [20] as in the active enzyme (Fig. 7). The two loops between the strands, however, are very different: a new type I  $\beta$ -bend is formed between Arg221A–Lys224 on activation of prethrombin2, whereas a

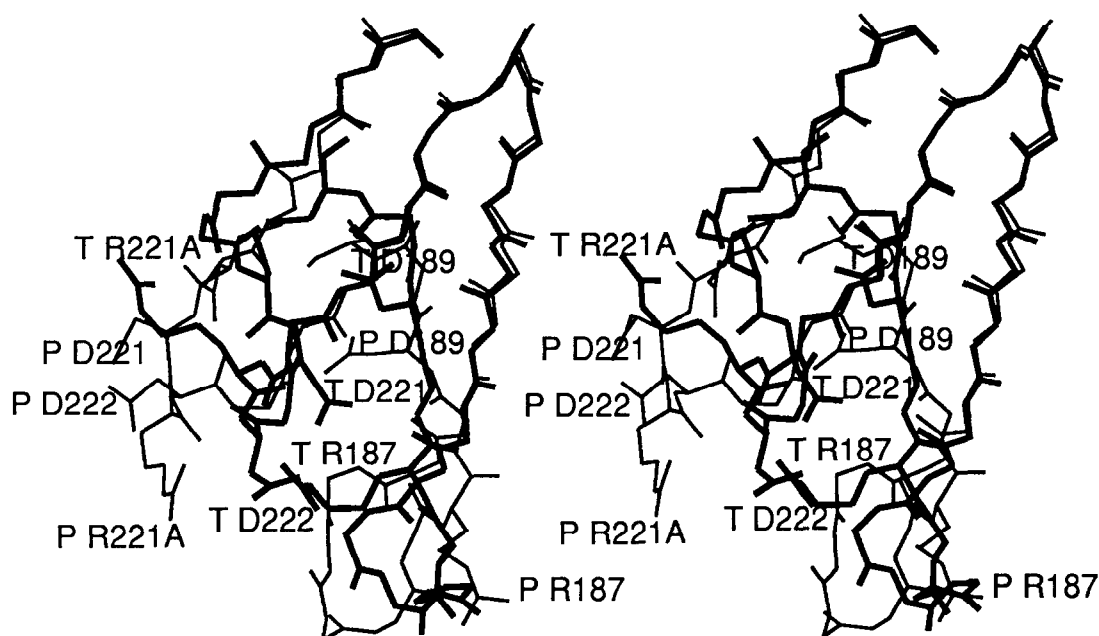


Fig. 7. Stereoview comparing the  $\text{Na}^+$  water channel of Hir-Throm and prethrombin2. Hir-Throm in bold; T and P designate thrombin and prethrombin2 residues respectively.

$\beta$ -turn between Asp186A–Lys186D of prethrombin2 is lost. A crucial driving force for these rearrangements is the formation of the bidentate salt bridge involving Arg187, Asp221 and Asp222. The positions of the side groups of the tripeptide Asp221–Asp222 region and that of Arg187 of prethrombin2 are inverted by the loop motions to form part of one entrance to the water channel (Fig. 7). The inversion also positions the carbonyl of Arg221A properly for interaction with a  $\text{Na}^+$  ion, and the encroachment of Asp221 on the sidechain of Asp189 of the specificity site causes it to shift and reorientate and anchor to Glu217O and Tyr228OH through hydrogen-bonding water molecules (Figs. 5 and 7). The motion of loop 1 on activation appears to be a simple pivot about Tyr184A and Lys186D. Thus, critical groups are not positioned correctly in prethrombin2 for the binding of either  $\text{Na}^+$  or the substrate, which is ultimately achieved by the triggering cleavage of the Arg15Ile16 bond [20].

### 3.8. $\text{Na}^+$ and $\text{K}^+$ sites in other proteins

Specific monovalent cation effects in proteins have been known for a long time [42–44]. The cations can

be allosteric effectors or cofactors that can interact directly or indirectly with substrates or can activate enzymes. Structures producing some of the effects have been determined for enzymes with specific requirements for  $\text{K}^+$  [45–47].

In dialkylglycine decarboxylase, there is a  $\text{K}^+$  site near the active center and a  $\text{Na}^+$  site on the protein surface at the carboxylate terminus of an  $\alpha$ -helix [45]. The former accounts for the dependence of activity on alkali metals. The exchange of  $\text{Na}^+$  for  $\text{K}^+$  results in a change in coordination geometry from octahedral to trigonal bipyramidal, with a reduction of metal–ligand distance from 2.7 to 2.3 Å. The surface  $\text{Na}^+$  site is formed by oxygen ligands from a reverse turn. In rabbit muscle pyruvate kinase, spherical electron density was assigned to  $\text{K}^+$  surrounded by four oxygen ligands [46]. However, it is 5.7 Å from the  $\text{Mn}^{+2}$  site, but an indirect linkage between the catalytic group and  $\text{K}^+$  may occur through hydrogen-bonded salt bridge interactions. Crystallographic anomalous scattering of  $\text{K}^+$  at 1.7 Å resolution revealed two  $\text{K}^+$  sites that interact with Mg ADP and Pi in the nucleotide binding cleft of bovine 70 kDa heat-shock cognate protein [47]. One  $\text{K}^+$  interacts with oxygen of the  $\beta$ -phosphate of

ADP whereas the other interacts with an oxygen of Pi. In crystals with Na<sup>+</sup>, K<sup>+</sup> is replaced at the former site and by a Na<sup>+</sup>–H<sub>2</sub>O pair at the other site. The K<sup>+</sup> are positioned so as to stabilize binding of a β, γ bidentate MgATP complex with the enzyme. All of the foregoing alkali metal ion binding sites are reminiscent of those of natural ionophores and synthetic macroscopic ligands [48–51]. If anything, variability and unpredictability of behavior underlie the protein interactions.

## Acknowledgements

This work was supported by NIH grant HL43229. We would also like to thank Professor Enrico Di Cera for numerous valuable discussions concerning the Na<sup>+</sup> binding site and for critically reading the manuscript.

## References

- [1] L.J. Berliner, Y. Sugawara and J.W. Fenton II, *Biochemistry*, 24 (1985) 7005.
- [2] J.-Y. Chang, P.K. Ngai, S. Dennis and J.-M. Schleepi, *FEBS Letters*, 261 (1990) 287.
- [3] T.J. Rydel, A. Tulinsky, W. Bode and R. Huber, *J. Mol. Biol.*, 221 (1991) 583.
- [4] W. Bode, D. Turk and A. Karshikov, *Protein Sci.*, 1 (1992) 426.
- [5] C.T. Esmon and W.G. Owen, *Proc. Natl. Acad. Sci. USA*, 78 (1981) 2249.
- [6] J.P. Sheehan, D.M. Tollefsen and J.E. Sadler, *J. Biol. Chem.*, 269 (1994) 32747.
- [7] T.K.H. Vu, V.I. Wheaton, D.T. Hung, I. Charo and S.R. Coughlin, *Nature*, 353 (1991) 674.
- [8] C.T. Esmon, R.C. Carroll and C.T. Esmon, *J. Biol. Chem.*, 258 (1983) 12238.
- [9] J. Hofsteenge, H. Taguchi and S.R. Stone, *Biochem. J.*, 237 (1986) 243.
- [10] X. Qiu, M. Yin, K.P. Padmanabhan, J.L. Krstenansky and A. Tulinsky, *J. Biol. Chem.*, 268 (1993) 20318.
- [11] I.I. Mathews, K.P. Padmanabhan, V. Ganesh, A. Tulinsky, M. Ishii, J. Chen, C.W. Turck, S.R. Coughlin and J.W. Fenton II, *Biochemistry*, 33 (1994) 3266.
- [12] I.I. Mathews, K.P. Padmanabhan and A. Tulinsky, *Biochemistry*, 33 (1994) 13547.
- [13] S. Konno, J.W. Fenton II and G.B. Villanueva, *Arch. Biochem. Biophys.*, 267 (1988) 158.
- [14] S.J.T. Mao, M.T. Yates, T.J. Owen and J.L. Krstenansky, *Biochemistry*, 27 (1988) 8170.
- [15] G.L. Hortin and B.L. Trimpe, *J. Biol. Chem.*, 266 (1991) 6866.
- [16] K.-P. Hopfner, Y. Ayala, Z. Szewczuk, Y. Konishi and E. Di Cera, *Biochemistry*, 32 (1993) 2947.
- [17] L.W. Liu, T.K. Vu, C.T. Esmon and S.R. Coughlin, *J. Biol. Chem.*, 266 (1991) 16977.
- [18] L.W. Liu, J. Ye, A.E. Johnson and C.T. Esmon, *J. Biol. Chem.*, 266 (1991) 23632.
- [19] J. Ye, N.L. Esmon, C.T. Esmon and A.E. Johnson, *J. Biol. Chem.*, 266 (1991) 23016.
- [20] J. Vijayalakshmi, K.P. Padmanabhan, K.G. Mann and A. Tulinsky, *Protein Sci.*, 3 (1994) 2254.
- [21] C.L. Orthner and D.P. Kosow, *Arch. Biochem. Biophys.*, 202 (1980) 63.
- [22] C.M. Wells and E. Di Cera, *Biochemistry*, 31 (1992) 11721.
- [23] Y. Ayala and E. Di Cera, *J. Mol. Biol.*, 235 (1994) 733.
- [24] A. Mathur, W. Schlappkohl and E. Di Cera, *Biochemistry*, 32 (1993) 7568.
- [25] Q.D. Dang, A. Vindigni and E. Di Cera, *Proc. Natl. Acad. Sci. USA*, 92 (1995) 5977.
- [26] E. Di Cera, E.R. Guinto, A. Vindigni, Q.D. Dang, Y.M. Ayala, W. Meng and A. Tulinsky, *J. Biol. Chem.*, 270 (1995) 22089.
- [27] E. Skrzypczak-Jankun, V.E. Carperos, K.G. Ravichandran, A. Tulinsky, M. Westbrook and J.M. Maraganore, *J. Mol. Biol.*, 221 (1991) 1378.
- [28] L. Lebeda and E. Zhang, *J. Appl. Cryst.*, 25 (1992) 323.
- [29] C.L. Orthner and D.P. Kosow, *Arch. Biochem. Biophys.*, 185 (1978) 400.
- [30] S.A. Steiner, G.N. Amphlett and F.J. Castellino, *Biochem. Biophys. Res. Commun.*, 94 (1980) 340.
- [31] K. Padmanabhan, K.P. Padmanabhan, A. Tulinsky, C.H. Park, W. Bode, R. Huber, D.T. Blankenship, A.D. Cardin and W. Kiesel, *J. Mol. Biol.*, 232 (1993) 947.
- [32] S.A. Steiner and F.J. Castellino, *Biochemistry*, 21 (1982) 4609.
- [33] P.C. Weber, L.-L. Lee, F.A. Lewandowski, M.C. Schadt, C.-H. Chang and C.A. Kettner, *Biochemistry*, 34 (1995) 3750.
- [34] C.S. Gibbs, S.E. Coutre, M. Tsiang, W.-X. Li, A.K. Jain, K.E. Dunn, V.S. Law, C.T. Mao, S.Y. Matsumura, S.J. Mejza, L.R. Paborsky and L.L.K. Leung, *Nature*, 378 (1995) 413.
- [35] D.K. Banfield and R.T.A. MacGillivray, *Proc. Natl. Acad. Sci. USA*, 89 (1992) 2779.
- [36] P.D. Martin, W. Robertson, D. Turk, R. Huber, W. Bode and B.F.P. Edwards, *J. Biol. Chem.*, 267 (1992) 7911.
- [37] M.T. Stubbs, H. Oschkinat, J. Mayr, R. Huber, H. Anglikar, S.R. Stone and W. Bode, *Eur. J. Biochem.*, 206 (1992) 187.
- [38] T.J. Rydel, M. Yin, K.P. Padmanabhan, D.T. Blankenship, A.D. Cardin, P.E. Correa, J.W. Fenton II and A. Tulinsky, *J. Biol. Chem.*, 269 (1994) 22000.
- [39] R.K. Arni, K. Padmanabhan, K.P. Padmanabhan, T.P. Wu and A. Tulinsky, *Biochemistry*, 32 (1993) 4727.

- [40] K. Padmanabhan, K.P. Padmanabhan, J.D. Ferrara, J.E. Sadler and A. Tulinsky, *J. Biol. Chem.*, 268 (1993) 17651.
- [41] K. Padmanabhan and A. Tulinsky, *Acta Cryst. D*, 52 (1996) 272.
- [42] P.D. Boyer, H.A. Lardy and P.H. Phillips, *J. Biol. Chem.*, 146 (1942) 673.
- [43] H.J. Evans and G.J. Sorger, *Annu. Rev. Plant Physiol.*, 17 (1966) 47.
- [44] C.H. Seutter, *Science*, 168 (1970) 789.
- [45] M.D. Tomey, E. Hohenster, S.W. Cowan and J.N. Jansonius, *Science*, 261 (1993) 756.
- [46] T.M. Larsen, L.T. Laughlin, H.M. Holden, I. Rayment and G.H. Reed, *Biochemistry*, 33 (1994) 6301.
- [47] S.M. Wilbanks and D.B. McKay, *J. Biol. Chem.*, 270 (1995) 2251.
- [48] M. Dobler, *Ionophores and their Structures*, Wiley, New York, 1981.
- [49] F. Vogtle and E. Weber (Eds.), *Host Guest Complex Chemistry: Macrocycles*, Springer, Berlin, 1985.
- [50] D. Cram, *Angew. Chem. Int. Ed. Engl.*, 25 (1986) 1039.
- [51] G. Eisenman and J.A. Dani, *Annu. Rev. Biophys. Biophys. Chem.*, 16 (1987) 205.